CHAPTER 91

LOADINGS ON LARGE PIERS IN WAVES AND CURRENTS

by

Hsiang Wang

University of Delaware, Newark, Delaware

Abstract

Through scale-model tests, the forces, moments, and the pressure distributions, including impact pressures, were determined for large diameter piers extending through large-amplitude wave system in which current strengths vary Tests were performed at 1/100 scale, simulating piers of the bridge for the Northumberland Strait Crossing, Canada These piers are partially cylindrical with a base diameter of 100 feet Close to the surface, where the wave action is greatest, they are conical Waves up to 25 feet and current up to 4 knots have been reproduced in the laboratory, according to Froude similitude The tests results fully support the known concept that, when the pier diameter is large in comparison with the wave length, inertial force becomes dominant Generally, the presence of current, either with or against the wave train, results in a decreasing wave force Semiempirical relations were developed for force predictions that require the experimental determination of a singular coefficient

Introduction

The problems of predicting wave forces on a cylindrical-shaped structure are often categorized according to the magnitude of the linear dimensions of the object and of the wave field Past advancement had been concerned mainly with the category of small-diameter cylinder under the action of small-amplitude waves (Morison et al , 1949, Goda, 1964, Bretschneider, 1955, 1957) Some attention has been given to the analytical treatment of the problem of a large-diameter pile (in comparison to the wave length) with small-amplitude wave (McCamy and Fuchs, 1954, Bonnefille and Germaine, 1963) These theories still remain to be verified by experiment When it comes to the problem of determining forces on a large-diameter cylinder protruding through a large-amplitude wave system, one quickly finds the lack of adequate information and reliable guidance The difficulty lay in general the lack of an adequate mathematical model on the one hand and the scarcity of experimental data on the other Therefore, the design of such a marine structure often presents a unique task of its own

The present study dealt with the prediction of wave forces on the piers of the bridge for the Northumberland Strait Crossing These piers are partially cylindrical with base diameter equal to 100 feet, close to the surface, where the wave action is greatest they are conical According to the information provided by the Northumberland Consultants, Ltd , the design storm is based on a 1 percent risk of occurrence once in 100 years resulting in wind of 95 mph on the northwest and southeast side of the crossing, respectively Significant wave of 14 foot height and 7 0 to 7 7 seconds is to be expected The extreme wave can be as high as 25 feet The design problem becomes unconventional Actually, this problem is further complicated because tidal current ranging from 0 to 4 knots is expected in the Strait This alters the wave kinematics and hence wave-induced forces Therefore, to obtain an engineering solution of this problem, once has little choice but to rely on the outcome of a scaled model test

This experimental investigation is intended to provide sufficient information to meet the immediate need of the specific design problem in hand and at the same time to serve as foundation and verification for the development of a possible theory It is realized that few model setups portray perfect dynamic similarity with their prototypes, and that, for all practical purposes, only the pertinent part of the phenomenon need be closely approximated As a result of dimensional analysis, it is not the viscous action, but wave inertia that is to be evaluated in the present instance Therefore, in addition to the absolute magnitude of the force and moment exerted on the structure, it is the above postulation with which the present investigation is concerned

Dimensional Analysis and Scaling Laws

The problem in hand is that of determining from experiments on a model of reduced scale the dynamic forces imposed by shallow water waves of relatively high amplitude upon a system of piers of partly cylindrical, partly conical shape An important aspect is that of determining the scaling laws to be applied

When an obstacle, such as a pier, is placed in the channel, it experiences a hydrodynamic force This force can be considered as consisting of two components respectively related to wave velocity and acceleration The velocity related force in the horizontal direction is given by

$$F(V,u) = \frac{1}{2} \pi \rho \int_{-d}^{\eta} C_d \quad [D(z)] \quad [V(z) + u(z)]^2 \, dz \tag{1}$$

where V is the current velocity, u is the horizontal component of the wave orbital velocity, ρ is the density of the water, d is the water depth, η is the wave ordinate, D is the diameter of the pier, z is vertical ordinate and C_d is a drag coefficient The drag coefficient is a function of, among other parameters, Reynold's number which is defined as

$$R = \frac{V D}{\nu}$$

where ν is the kinematic viscosity The acceleration related force is given by

$$F(u) = \frac{\pi \rho}{4} \int_{-d}^{\eta} C_1 \quad [D(z)]^2 \quad [\dot{u}(z)] \, dz \tag{2}$$

where C_1 is an inertia coefficient which depends mainly on the Ursell number

$$U_n(z) = \frac{4\pi^2 D(z)}{gT^2} = \frac{D(z)}{L}$$

The Ursell number is actually an inversed Froude number preferred in wave mechanics

The foregoing argument leads to the point that dynamic similarity requires that both Froude and Reynold's numbers be preserved Since simultaneous Froude and Reynolds scaling of reduced model is impossible, a choice must be made To this end it is brought out that the ratio of the acceleration force to the velocity force at any level of the pier is

$$\frac{\pi C_1 \quad D(z)}{C_d \quad H(z)}$$

and since the inertia and drag coefficients are of approximately equal value, the ratio reduces to $\pi D(z)/H(z)$ This ratio is always greater than unity even for the waves of extreme height and in the cylindrical portion of the pier much greater than unity, so that the acceleration force dominates the velocity force and the resultant hydrodynamic force is close to the acceleration components The consequence of this is that the scaling should follow the Froude law

The integration of Eq (2), which represents the acceleration component of the hydrodynamic force, cannot be carried out unless explicit expressions of C_1 and u can be obtained The other alternative is to establish the functional relationship through dimensional analysis between this force component and other pertinent fluid, flow, and geometrical variables. By the latter method the following relation is obtained

$$\frac{F/(D^2 d)}{\rho \; H/T^2} = E_n \left(\frac{D}{L}, \frac{VT}{D}, \frac{H}{d}, \frac{V}{(gd)^{1/2}} \right) \tag{3}$$

Where E_n is a modified Euler number which represents a force coefficient, and T is the wave period, H is the wave height, and g is the gravitational acceleration

Evidently the number of parameters involved makes a thorough investigation burdensome, further simplification is desirable McCamy and Fuchs (1955) obtained analytically the amplitude of the wave force per unit height acting on a cylinder at depth z below the surface as

$$F(z) = \frac{\rho \; H \; L}{\pi} \quad \frac{\cosh\,[2\pi(z+d)/L}{\cosh 2\pi d/L} \quad f_A \tag{4}$$

where

$$f_A = \left[\frac{1}{[J_1'(\pi D/L)]^2 + [Y_1'(\pi D/L)]^2}\right]^{1/2}$$

and J_1 and Y_1 are Bessel functions of the first and the second kinds, respectively, and the prime denotes first derivative Accordingly the total force is

$$F = \int_{-d}^{\eta} F(z)dz = \frac{\rho H}{\pi} \frac{L^3}{T^2} f_A \tag{5}$$

When $\pi D/L$ is small,

$$f_A \sim (\frac{\pi}{2}) (\pi D/L)^2$$

$$\text{and } F \sim \frac{\pi^2}{4} \frac{\rho H}{T^2} L D^2 \tag{6}$$

On the other hand, when $\pi D/L$ is large,

$$f_A \sim (\frac{1}{2})^{1/2} \pi (\frac{D}{L})^{1/2}$$

and

$$F \sim \sqrt{1/2} \frac{\rho H}{T^2} L^{5/2} D^{1/2} \tag{7}$$

Physically, the last two equations imply that when D/L is small, the pier diameter is the controlling factor, whereas, when D/L is large, the effect of wave length becomes predominant The present pier-diameter-to-wave-length ration ($\pi D/L$ ranges from 1 to 1 5) is believed to fall into the latter category The force coefficient is redefined as

$$\frac{F/(L^{5/2} D^{1/2})}{\rho H/T^2} = C_m = C_m (\frac{VT}{D}, \frac{H}{d}, \frac{V}{(gd)^{1/2}}) \tag{8}$$

For the case of shallow water, this equation simplfied further to

$$\frac{F}{g^{5/4}\rho HT^{1/2}D^{1/2}d^{5/4}} = C_{ms} = C_m (\frac{VT}{D}, \frac{H}{d}, \frac{V}{(gd)^{1/2}}) \tag{9}$$

The parameter VT/D is a Strouhal number written in the form preferred by Keulegan and Carpenter (1958), in the case of combined wave and current the more appropriate expression is $[V + U_m]T/D$, where U_m is the maximum horizontal particle velocity in the wave This parameter characterizes the wake and eddy formations and is thus more directly related to viscous forces It has been shown that, in the present case, the viscosity plays a minor role Therefore, it is expected that the effect of the parameter on the force coefficient is insignificant In fact, the value of $[V + U_m]T/D$ varies from 1 to 3 for the range of variables in the present experiment Keulegan and Carpenter were able to show that for the parameter as small as such no eddy shedding occurs Consequently, the force coefficient remains practically constant Finally, the force relation is simplified to

$$\frac{F}{g^{5/4}\rho H T^{1/2} D^{1/2} d^{5/4}} = C_{ms}\left(\frac{H}{d}, \frac{V}{(gd)^{1/2}}\right) \tag{10}$$

Experimental Apparatus and Procedure

Facility

The experimental study was carried out in the wave tank shown in Fig 1 Stable waves of steep profile and of period ranging from 0 74 to 4 seconds for water depths as shallow as 6 inches can be generated at the test section Current corresponding to controlled rates ranging from 500 to 4000 gpm can be developed either in or against the direction of wave propagation A current deflector is fitted in way of the ports in the converging section to reduce the up-swelling action of the flow entering from the ports A spending beach of 1 20 slope is installed at the end opposite from the wave generating section, to reduce wave reflection and to smooth the velocity distribution when the current is made to flow opposite the wave direction

Pier Model

The pier model (Fig 2) is made of aluminum at a scale of 1/100 that of the prototype It consists of four detachable sections so that, as water depth is varied, the position of the calm waterline remains relatively unchanged and approximately 1 5 to 2 inches above the top of the cylincrical portion of the pier The pier model is fitted with three adaptors for diaphragm-type pressure transducers, two in the conical section and one in the uppermost section of the cylindrical body Each cylindrical section of the model is also tapped for cavity-type pressure transducers Generally, pressure transducers are sensitive to temperature fluctuations When the pressure fluctuations to be measured are small, as in the present tests, temperature fluctuations can have a pronounced effect on the results To minimize the possible error so introduced, the temperature of the transducers is matched to that of the water in the tank by continuously running a thin film of tank water over the transducers

Two force gages are mounted to a 2-inch by 1/4-inch flat bar which is fixed on the side wall of the wave tank and protrudes into the pier through the opening at its top These gages are for the measurement of the magnitude and point of application of the horizontal hydrodynamic force exerted on the pier The lower gage is fixed to its flat-bar support and allowed to float in a force-transmitting adaptor which is fixed

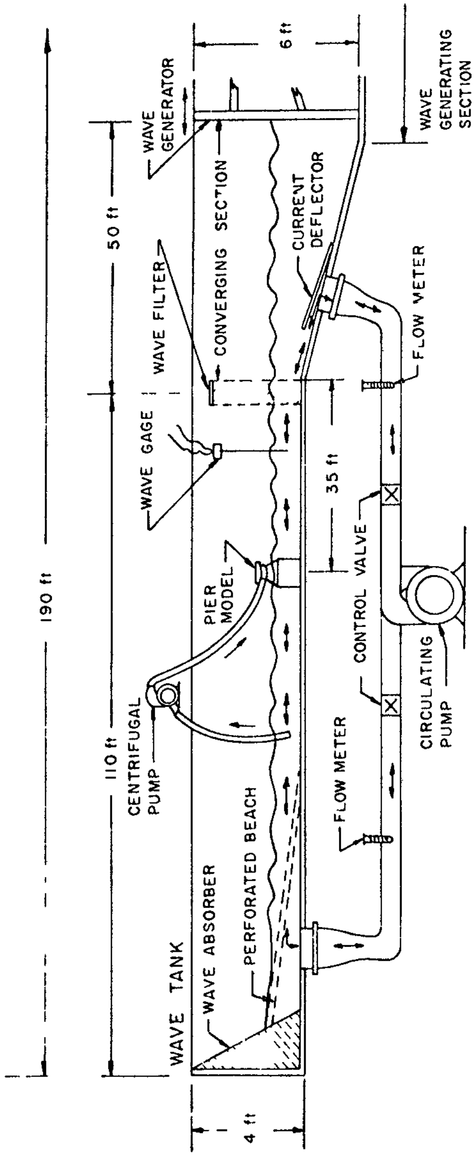

Figure 1
General Arrangement of Experimental Setup

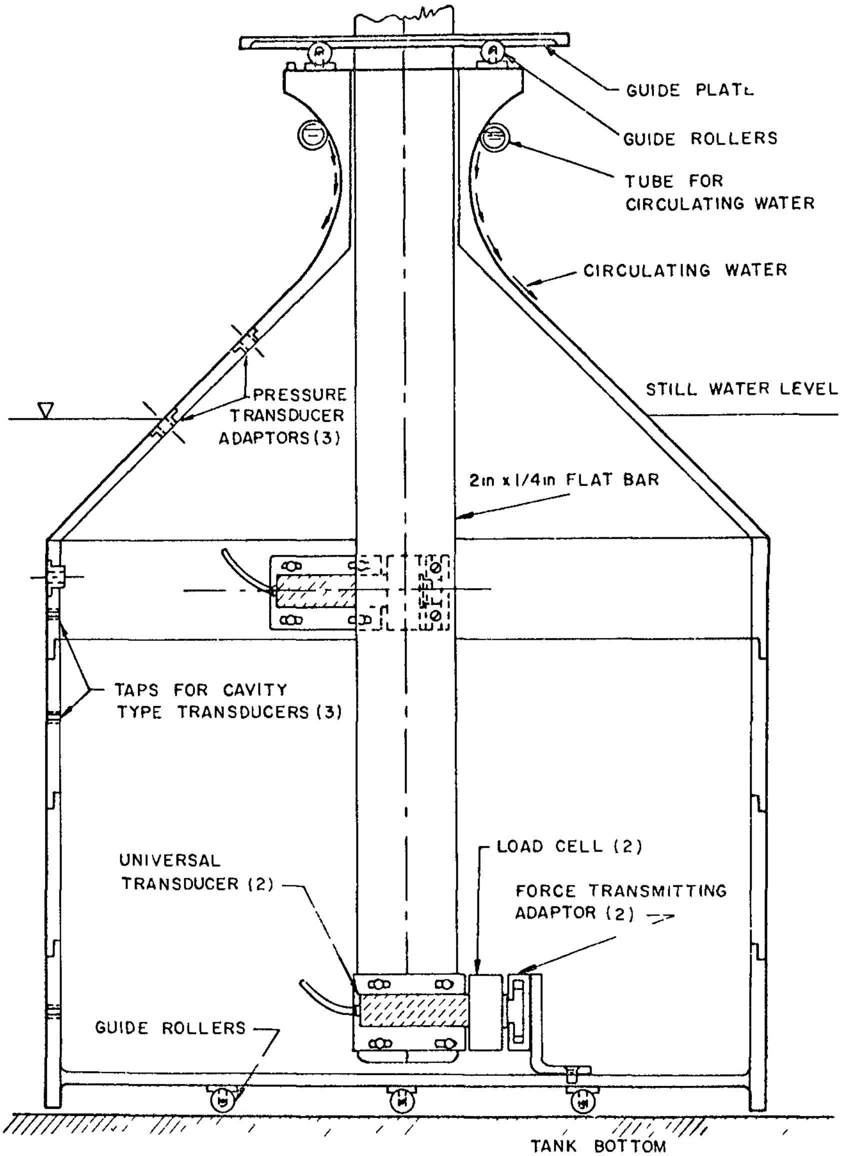

Figure 2

Pier Model

to the pier and designed to transmit only tension or compression in the horizontal direction The upper gage is mounted in a reverse fashion, it is fixed to the pier and allowed to float in an adaptor fixed to the flat bar (Fig 2)

Instrument

The flush diaphragm pressure transducers and the cavity pressure transducers are both of the resistive type and manufactured by Statham Instruments, Inc The former, with a pressure range of 0 to 5 psig and a natural frequency of 3 5 KC, are used to measure the wave pressure on the pier in the region where waterline fluctuates and impact is likely to happen, whereas the latter, with a pressure range of 0 5 psi differential pressure, are used in the region that is always fully submerged

The force gage consists of a Statham Universal Transducing Cell of Model UC3 and a load cell adaptor with a load range of 50 pounds The Universal Transducing Cell is itself a basic sensing element made from strain gages and is capable of measuring a variety of physical parameters by using different adaptors The load cell adapter is, of course, as its name implies, an accessory for transmitting forces

The water surface elevations were measured by resistance type gage consisting of a pair of surface-piercing parallel wires, across which an excitation voltage was impressed The corresponding voltage variations caused by fluctuations of the wetted line on the gage were recorded in wave-forms on a paper by a Sanborn Recorder

The current-velocity distributions across the test section were measured by conventional 0 25-inch Pitot tubes in conjunction with precision manometer which can be read to 0 001 inch

Procedure

The magnitude and point of application of the horizontal force were determined for the various combinations of wave and current characteristics of Table 1 In these tests, the model of the pier was first made quasi-neutrally buoyant by ballasting The model was then suppressed into the water by a horizontal bar mounted fixed to the side wall of the tank, but clear of the tank bottom Guide rollers between the model and the bar confined the pier model to move in the horizontal direction The force gages were mechanically biased to one-half of their full range so that they would respond in both tension and compression to a 25-pound maximum value These gages were calibrated by applying through a set of pulleys known horizontal forces at the midpoint between gages

The hydrodynamic pressure distribution was also determined for the combination of wave and current characteristics of Table 1 and for water depths of 6 inches and 12 inches corresponding to 50 and 100 foot full scale In these tests, the model of the pier was mounted so as to be

TABLE 1

Test Schedule for Force and Pressure Measurement

Water Depth	Model (in)	6	9	12
	Prototype (ft)	50	75	100
Current Speed	Model (fps)	0, ± 0 2, ± 0 4, ± 0 6	0, ± 0 2, ± 0 4, ± 0 6	0, ± 0 2, ± 0 4, ± 0 6, ± 0 8
	Prototype (Knots)	0, ± 1 2, ± 2 4, ± 3 6	0, ± 1 2, ± 2 4, ± 3 6	0, ± 1 2, ± 2 4, ± 3 6, ± 4 8
Wave Height	Model (in)	1 4 3 0	1 4 3 0	1 4 3 0
	Prototype (ft)	12 25	12 25	12 25
Wave Period	Model (sec)	0 75, 0 85, 1 0	0 75, 0 85, 1 0	0 75, 0 85, 1 0
	Prototype (Sec)	7 5, 8 5, 10	7 5, 8 5, 10	7 5, 8 5, 10

fixed to the tank The pressure was measured at five points along a meridan Measurements were made for 30-degree increments in polar angle with respect to current and wave direction

The impact pressure was sensed by transducers of the flush diaphragm type since in the region of impact the transducer is alternately wet and dry Because of the short duration of the impact, the signal transmitted by the transducer, after being amplified, was displayed on an oscilloscope and photographically recorded

Test Results and Discussion

Wave Force

A typical time record of the wave force exerted on the pier along with the history of the wave measured alongside the pier is shown in Fig 3 From these records it is possible to determine the phase of the wave, with reference to the centerline of the pier, at which the wave force is a maximum This maximum occurs when the wave node coincides with such centerline, for which condition the velocity-dependent force is a minimum Thus, the maximum wave force is almost solely of acceleration-induced loading This result supports the argument made under Dimensional Analysis and Scaling Laws

It has been shown that the force coefficient defined in Eq (2) is a function of the H/d and $V/(gd)^{1/2}$ The effect of wave steepness (H/d) on the force coefficient is found to be insignificant, at least in the tested range of H/d (0 08 - 0 4)

In the case of shallow water, in the present experiment, the parameter $V/(gd)^{1/2}$, which is the determining the influence of current on wave kinematics, although just how this parameter is related to wave dynamics is, as yet, somewhat unexplained The experimental results of C_{ms} plotted versus $V/(gd)^{1/2}$, are shown in Figs 4, 5, and 6 for water depths of 6, 9, and 12 inches respectively The heavy solid lines in these figures are based on averaged values The force coefficient fluctuates in the region of positive $V/(gd)^{1/2}$ A reverse current of increasing strength, however, always results in smaller force The values of $V/(gd)^{1/2}$ which corresponds to maximum C_{ms} fall in the region of 0 to 0 25

The foregoing arguments lead to the point that the wave force acting on the (full scale) pier can be calculated from

$$F = C_{ms}\ \rho g^{5/4} H T^{1/2} D^{1/2} d^{5/4}$$

where C_{ms} has to be determined by model test at the corresponding Froude number The wave height H is the local wave height with the absence of the pier and the current

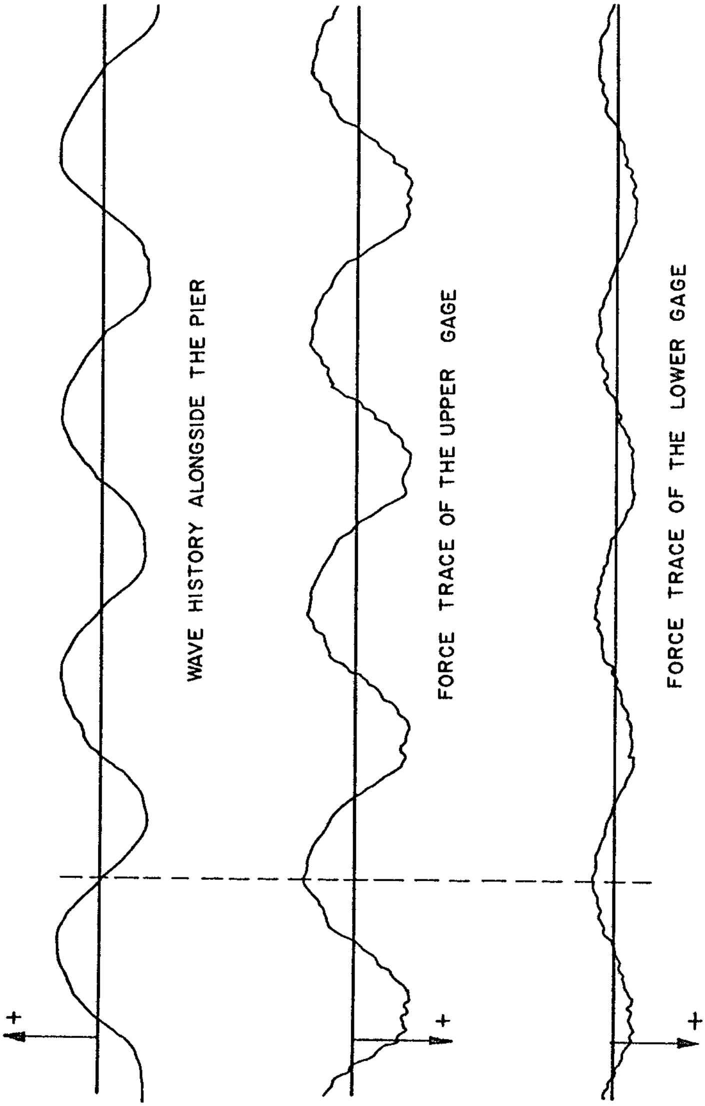

Figure 3
Example of Time Record of Force Measurement

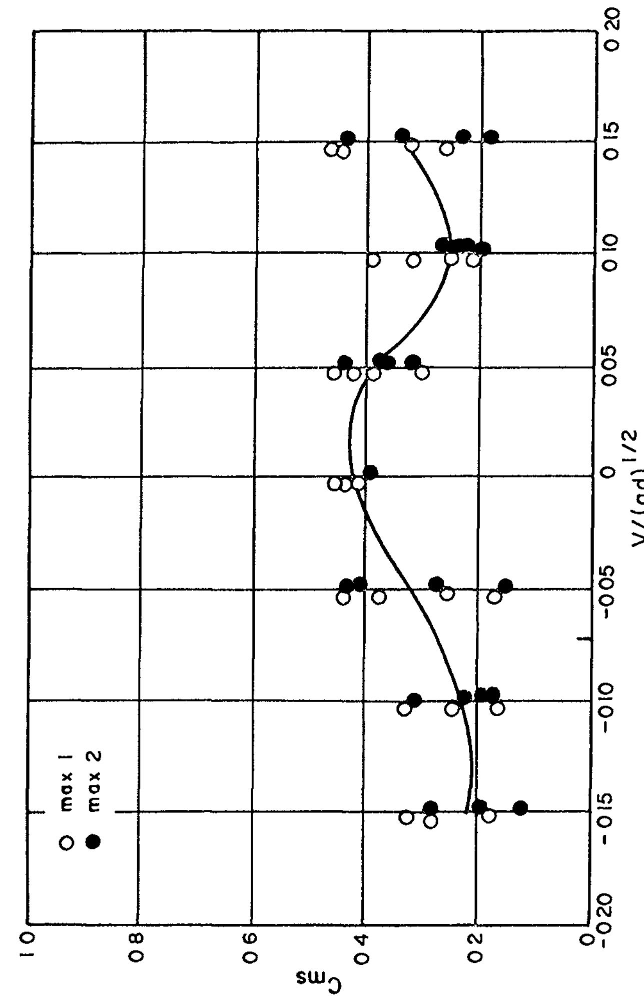

Figure 4
Force Coefficient versus Current Strength (d = 6 inches)

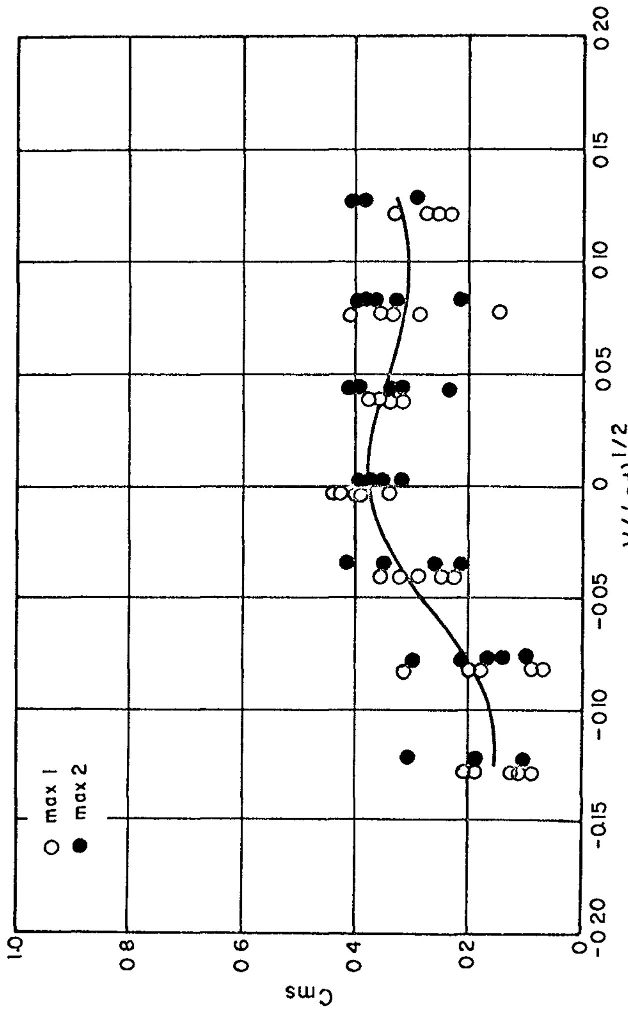

Figure 5

Force Coefficient versus Current Strength (d = 9 inches)

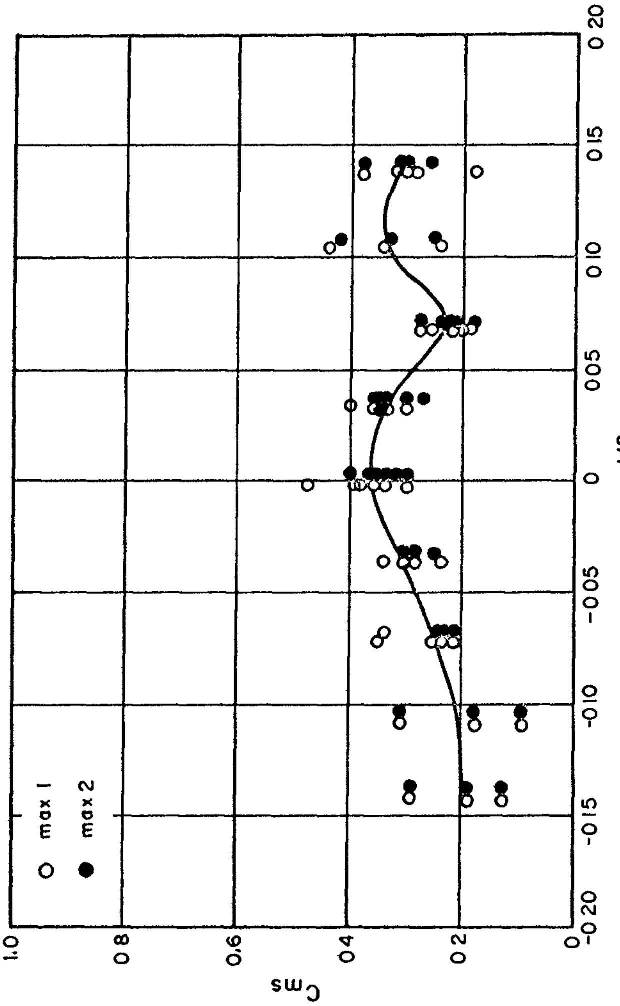

Figure 6
Force Coefficient versus Current Strength (d - 12 inches)

The wave force so obtained were generally larger than those computed by using the linear diffraction theory developed by McCamy and Fuchs (of the order of 20 - 30 per cent) It is also noted here that the experimental study dealt with a case of two-dimensional simulation in that the pier model was placed and tested in the middle of a straight channel which is approximately 40 feet away from either end of the current inlets This arrangement discounted the effects of channel constriction near which wave and current encounters and the flow is either accelerated or decelerated depending on the flow directions Experimental results reveal that the wave height at the test section with the absence of the pier model is always diminished by the effect of the current As a consequence, the greatest hydrodynamic loading exerted on the pier is obtained when the current is null, since the wave force is directly proportional to the wave height

However, one must be cautious to extend this conclusion to cases where three-dimensional effects mentioned above might be pronounced In fact, additional experiments were conducted in the tank and demonstrated that for long waves in shallow water the wave height was augmented by an oppose current

The point of application of the maximum horizontal force does not vary appreciably with change in test condition The mean values of the point of application measured from the mud line and their standard deviations are listed below

Water depth (d) (Inch)	Mean ($\frac{z}{d}$)		Standard deviation	
	Max 1	Max 2	Max 1	Max 2
12	0 535	0 525	0 049	0 055
9	0 585	0 555	0 053	0 073
6	0 575	0 550	0 085	0 098

The Max 1 and Max 2 are defined as in Fig 8

Wave Pressure

Pressure distribution about the pier was measured for water depths of 6 and 12 inches The pressure characteristics for both cases are quite similar Experimental results for the case of 12-inch depth only are presented here for the purpose of discussion Figure 7 illustrates the instantaneous pressure about the pier at a certain vertical position Figure 8 summarizes the results of maximum pressures as a function of angular and vertical position

The gross characteristics of the pressure about the pier model does not differ significantly from the case of a straight circular cylindrical caisson in the absence of current (Laird, 1955) - i e , neither the shape of the distribution curve nor the magnitude of the peak value ap-

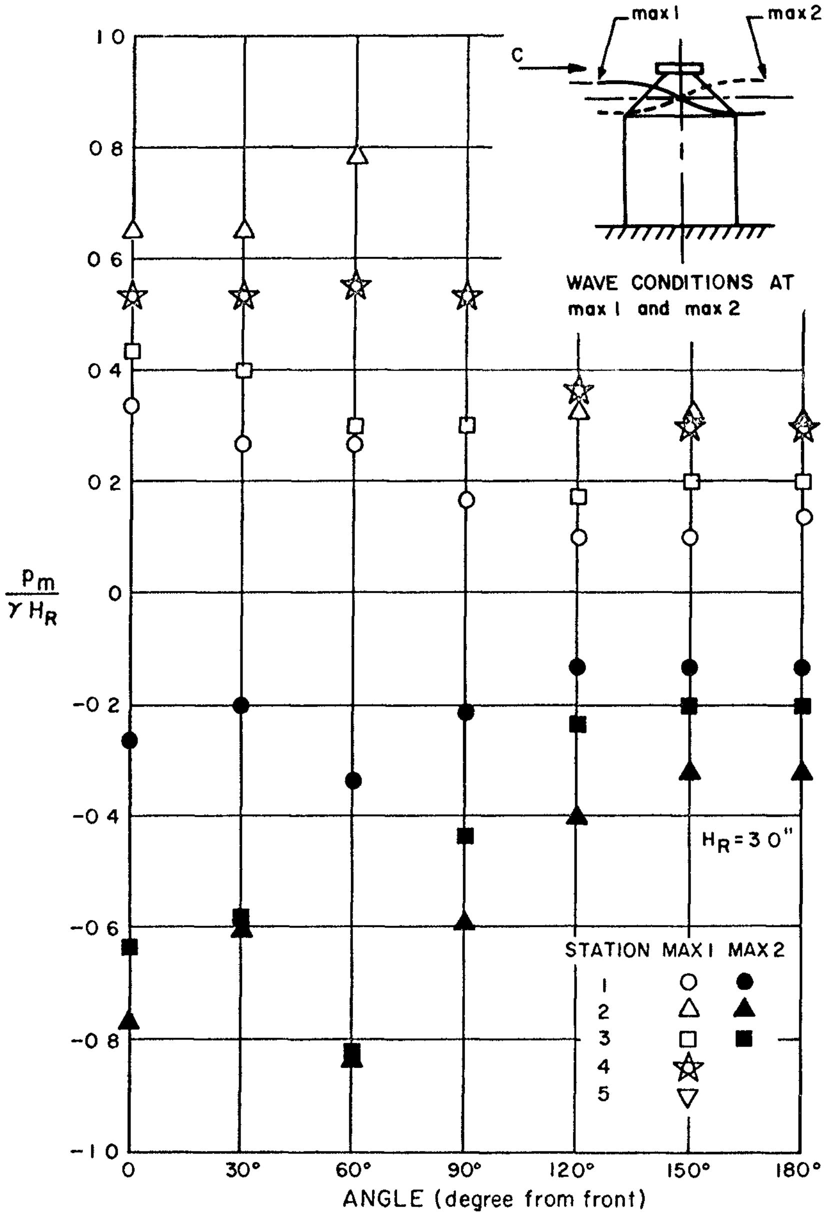

Figure 7

Pressure About the Pier at a Vertical Section

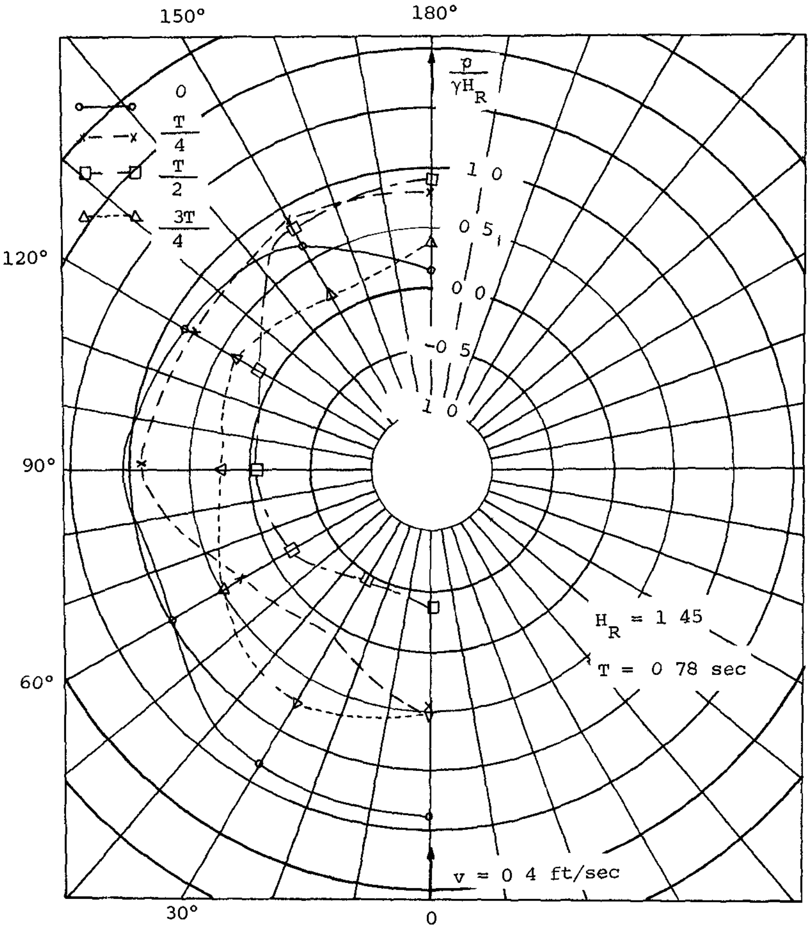

Figure 8

Maximum Pressures as a Function of Angular and Vertical Position
(V = -0 2 ft/sec)

peared abnormal with respect to the case of straight caisson The effects of the conical upper section of the pier model are two fold (1) The wave pressure on this section itself is reduced considerably in comparison with that on a circular cylinder of comparable base diameter (2) The pressure on the cylindrical portion, immediately below the tapered section is also reduced, possibly due to the greatly reduced reflection by the conical section

Note that the maximum pressure amplitude occurs either at or close to the forward stagnation point (facing waving and current) and is slightly smaller, or at most equal to, than that corresponding to a change in level equal to the wave height This means that the wave is almost completely reflected by the cylindrical portion of pier

The current affects the pressure distribution on the pier in the same manner as it affects the horizontal force, the magnitude of the maximum pressure fluctuates for increasing strength of forward current but decreases for increasing strength of opposed current To a certain extend the presence of the current tends to deflect the wave front when waves approach the pier This effect causes the location of the maximum pressure to shift away from the stagnation point

The wave force exerted on the pier in the horizontal direction can also be obtained by integrating the pressure around the pier according to the following equation

$$F = \int_0^{\eta(\theta)} dz \int_0^{2\pi} \frac{D(z)}{2} p(\theta,z) \cos\theta \cos\beta \, d\theta$$

or

$$F = \gamma D H_R \int_0^{\eta(\theta)} dz \int_0^{\pi} \frac{D(z)}{D} \frac{p(\theta,z)}{\gamma H_R} \cos\theta \cos\beta \, d\theta$$

where θ is the azimuth angle and β is the angle of normal of the surface measured from mud line As an example, the maximum horizontal force for a specific case of H_R = 1 45 inch and V = 0 ft/sec was computed graphically and compared with the result of direct measurement Upon graphical integration values of

$$\int_0^{\pi} \frac{D(z)}{D} \frac{p(\theta,z)}{\gamma H_R} \cos\theta \cos\beta \, d\theta$$

are obtained These values when plotted versus the height of pier (Fig 9) can be used to construct the horizontal load distribution diagram on the

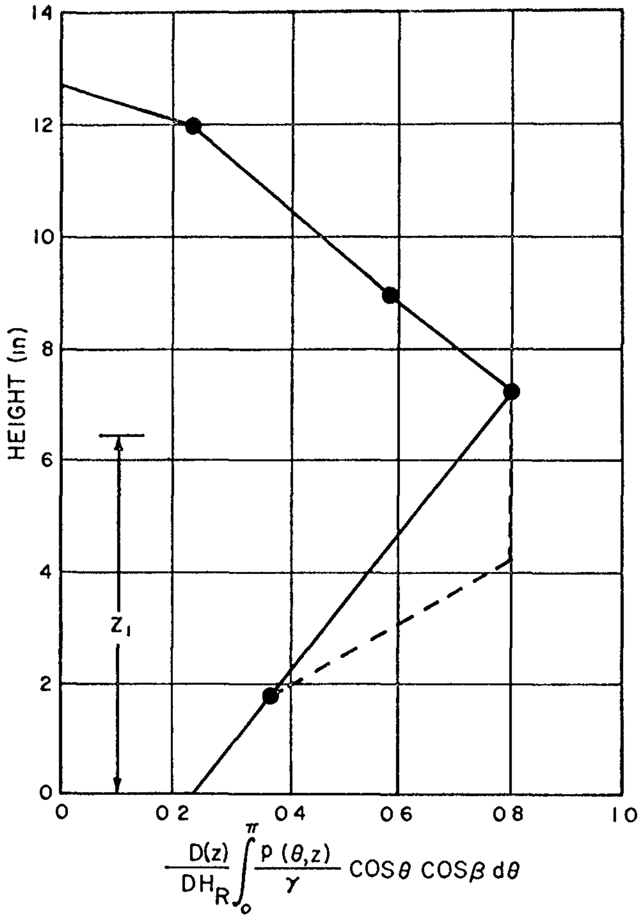

Figure 9

Load Diagram on Pier

pier The magnitude and the point of application of the total force calculated according to the force diagram which connects the data points by straight lines are respectively, 4 85 pounds and 6 4 inches The corresponding values in the direct measurement are 5 4 pounds and 6 3 inches The force magnitude obtained from pressure integration is 15 per cent smaller than directly measured This error results from the over simplified load diagram A more realistic, yet still simply constructed, load diagram is proposed and shown by the dotted line According to this modified load diagram, the magnitude and the points of application of the resultant force become 5 4 pounds and 6 1 inches

The load diagram also reveals two facts (1) A predominate portion of the total load applies on the middle section of pier Thus the point of application becomes insensitive to the variation of load magnitude This fact was observed and noted in the direct-force measurement (2) The horizontal load on the conical section contributes merely 10 per cent to the total load This leads to the explanation that the point of application of the horizontal force in the present geometrical configuration is considerably lower than that of a straight cylindrical cassion

Impact Pressure

With regard to the impact pressure measurement, Fig 10 shows a typical pressure traces displayed on the oscilloscope In the region of the upper tapered section, no impact was ever observed In the upper portion of the cylindrical section, impact of moderate magnitude (generally smaller than the maximum dynamic pressure) was observed occasionally when the backwash from the tapered section met the oncoming wave It was concluded that, for the present test conditions, the waves are neither steep enough or fast enough to induce significant impact loadings

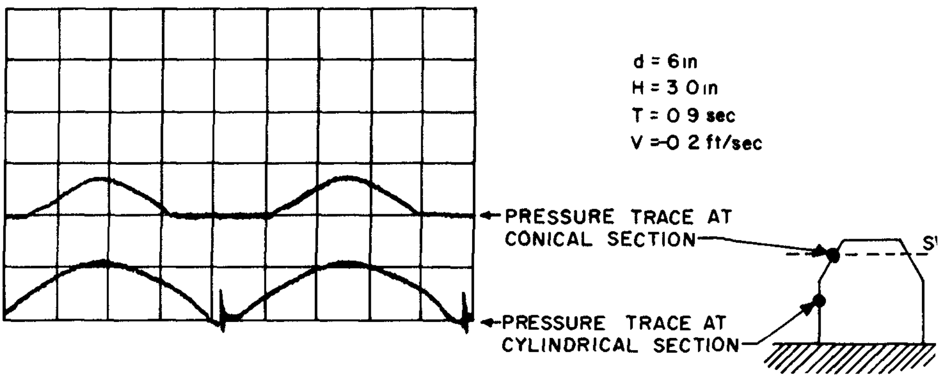

Figure 10

Examples of Time Record of Impact Pressure Measurement

Conclusions

Through scaled-model tests, the forces, moments, and the pressure distributions on the piers of the bridge for the Northumberland Strait Crossing have been determined Geometrical simulations were partially fulfilled by placing the pier model in a wave channel that has a width of 4 feet The test results fully support the known concept that when the pier diameter is large in comparison with the wave length, wave inertial force becomes predominant Generally, the presence of current in either direction results in a decreasing in wave force unless the pier is located at the channel entrance where a relatively long wave encounters a strong current in a shallow water

As far as the wave force is concerned, the conical pier section serves three functions the total horizontal force is considerably reduced, the point of application of the horizontal force is lowered and becomes insensitive to the wave height, and the danger of wave impact is removed

Measurements conducted in the wave tank provided the single experimental coefficient required to complete the result of dimensional analysis for this case This coefficient is reasonably well behaved for a range of current strength and wave parameters Consequently, all results reported herein are considered applicable for design purposes to bridge piers and to structures of similar geometry

Acknowledgement

The program was sponsored by the Northumberland, Ltd of Canada The permission of publication by the Department of Public Works of Canada is gratefully acknowledged The author is also indebted to Dr Manley St Denis for his contribution and Drs Thomas Monti, and Ean Ma Caig, and Messrs Carlo Pentassuglia and James Cowley for their fruitful discussion

References

Bonnefille, R and Germain, P , "Wave Action on Isolated Vertical Cylinders of Large Dimensions," I A H R Congress, London, 1963

Bretschneider, C L (1955), "An Evaluation of Inertia Coefficients in Wave Forces Experiments," Texas A & M Research Foundation Tech Report No 55-2

Bretschneider, C L (1957), "Evaluation of Drag and Inertia Coefficients for Maximum Range of Total Wave Forces," Texas A & M Research Foundation Report No 55-5

Goda, Y (1964), "Wave Forces on a Vertical Circular Cylinder," Port and Harbour Technical Research Institute, Japan, Report No 8

Keulegan, Garkis H , and Carpenter, Lloyd H (1958), "Forces on Cylinders and Plates in an Oscillating Fluid," Journal of Research, National Bureau of Standards, 60, 5, May 1958

Laird, A D K (1955), "A Model Study of Wave Action on a Cylindrical Island," Transition American Geophysical Union, 36, 2 April 1955

Longuet-Higgins, M S and Stewart, R W (1961), "The Changes in Amplitude of Short Gravity Waves on Steady Non-uniform Current," Journal of Fluid Mechanics, 10, part 4, June 1961

MacCamy, R C , and Fuch, R A (1954), "Wave Force on Piles, a Diffraction Theory," U S Army Corps of Engineers, Beach Erosion Board, Technical Memorandum No 69, December 1954

Morison, J R , Johnson, J W and O'Brine, M P (1953), "Experimental Studies on Forces on Piles," Proceedings of Fourth Conference on Coastal Engineering